

Measuring Utility and Privacy of Synthetic Genomic Data

Bristena Oprisanu UCL bristena.oprisanu.10@ucl.ac.uk	Georgi Ganev UCL and Hazy georgi.ganev.16@ucl.ac.uk	Emiliano De Cristofaro UCL and Alan Turing Institute e.dechristofaro@ucl.ac.uk
--	---	--

Abstract

Genomic data provides researchers with an invaluable source of information to advance progress in biomedical research, personalized medicine, and drug development. At the same time, however, this data is extremely sensitive, which makes data sharing, and consequently availability, problematic if not outright impossible. As a result, organizations have begun to experiment with sharing *synthetic* data, which should mirror the real data’s salient characteristics, without exposing it. In this paper, we provide the first evaluation of the utility and the privacy protection of five state-of-the-art models for generating synthetic genomic data.

First, we assess the performance of the synthetic data on a number of common tasks, such as allele and population statistics as well as linkage disequilibrium and principal component analysis. Then, we study the susceptibility of the data to *membership inference attacks*, i.e., inferring whether a target record was part of the data used to train the model producing the synthetic dataset. Overall, there is no single approach for generating synthetic genomic data that performs well across the board. We show how the size and the nature of the training dataset matter, especially in the case of generative models. While some combinations of datasets and models produce synthetic data with distributions close to the real data, there often are target data points that are vulnerable to membership inference. Our measurement framework can be used by practitioners to assess the risks of deploying synthetic genomic data in the wild, and will serve as a benchmark tool for researchers and practitioners in the future.

1 Introduction

Progress in genome sequencing is helping pave the way towards prevention, diagnosis, and treatment of several diseases and conditions. Much of this progress is dependent on the availability, and consequently the sharing, of genomic data. Numerous initiatives have been established to support and encourage genomic data sharing, and funding agencies like the National Institutes of Health (NIH) often make it a requirement to fund grant applications [42]. Successful data sharing programs include the International HapMap Project [38], which helped identify common genetic variations and study their involvement in human health and disease, as well as the 1000 Genomes Project [4], which aims to create a catalog of human variation and genotype data.

Overall, data sharing in genomics is crucial to enable progress in Precision Medicine [21]. Unsurprisingly, however, this is inherently at odds with the need to protect individuals’ privacy. Genomic data contains sensitive information related to heritage, predisposition to diseases, phenotype traits, etc., which makes it hard to anonymize [23]. Hiding “sensitive” portions of the genome is not effective either, as sensitive information can still be inferred via high-order correlation models [48]. For a thorough review of privacy threats in genomics, please see [8, 40, 59].

As a result, genomics researchers have begun to investigate the possibility of releasing *synthetic* datasets, rather than real/anonymized data [46]. This follows a general trend in healthcare; for instance, the National Health Service (NHS) in England has recently concluded a project focused on releasing synthetic Emergency Room (“A&E”) records [41]. The intuition is to use generative models to learn to generate samples with the same characteristics—more precisely, with the same distribution—of the real data. That is, rather than releasing data of actual individuals, entities share artificially generated data in such a way that the statistical properties of the original data are preserved, but minimizing the risk of malicious inference of sensitive information [16].

Generative Models and Genomics. Specific to genomics, previous work has experimented with both statistical and machine learning generative models. Samani et al. [48] propose an inference model based on the recombination rate, which can also be used to generate new synthetic samples. Yelmen et al. [61] use Generative Adversarial Models (GANs) and Restricted Boltzmann Machines (RMBs) to mimic the distribution of real genomes and capture population structures. Finally, Killoran et al. [33] use ad-hoc training techniques for GANs and architectures for computer vision tasks.

Motivation. Prior work on generating synthetic data in genomics has thus far only scratched the surface with respect to assessing their utility, and more specifically their statistical fidelity. Moreover, we do not really know whether these approaches

actually provide any meaningful privacy guarantees. To address this gap, we introduce a novel evaluation framework and perform a series of measurements geared to assess both the utility and the privacy of five state-of-the-art models used to generate human genomic synthetic data. More specifically:

- *Utility.* We focus on a number of very common computational tasks on genomic data. We measure how well generative models preserve summary statistics (e.g., allele frequencies, population statistics), or linkage disequilibrium. We also assess how close are the distributions of synthetic data vs. real data for principal component analysis.
- *Privacy.* We mount *membership inference attacks* [29], having an attacker infer whether a target record was part of the real data used to train the model producing the synthetic dataset. More precisely, we quantify the privacy gained, vis-à-vis this attack, from releasing synthetic data vs. releasing the real dataset. In the process, we also introduce a novel attack where the adversary only has *partial* information for a target individual.

Main Findings. Overall, our evaluation shows that there is no single approach for generating genomic synthetic data that performs well across the board, both in terms of utility and privacy. However, some models, provide high utility as well as increased privacy protection. Among other things, we find that:

- A high order correlation model (Recomb) has the best utility metrics for small datasets, but does so at the cost of privacy, even against weaker adversaries who only have partial information available.
- The RBM model has a better performance with increasing dataset sizes, both in terms of utility and privacy, as more targets benefit from privacy gain when synthetic data is generated using a larger training set.
- There are combinations of target and training sets for which releasing the synthetic dataset increases the privacy loss, but one cannot meaningfully predict what these combinations will be without actually running the privacy evaluation part of our framework.

2 Preliminaries

In this section, we introduce background information about genomics, then, we present the privacy metrics and datasets used in our evaluation.

2.1 Genomic Primer

Genomes and Genes. The genome represents the entirety of an organism’s hereditary information. It is encoded in DNA (deoxyribonucleic acid); each DNA strand is made up of four chemical units, called nucleotides, represented by the letters A, C, G, and T. The human genome consists of approximately 3 billion nucleotides, that are packaged into thread-like structures called chromosomes. The genome includes both the genes and the non-coding sequences of the DNA. The former determine specific traits, characteristics, or control activity within an organism. We refer to the group of genes that were inherited together from a single parent as a *haplotype*. An *allele* is a different variation of a gene; any individual inherits two alleles for each gene, one from each of their parents. The genotype consists of the alleles that an organism has for a particular characteristic.

SNPs and SNVs. About 99.5% of the genome is shared among all humans; the rest differs due to genetic variations. Single nucleotide polymorphisms (SNPs) are the most common type of genetic variation. They occur at a single position in the genome and in at least 1% of the population. SNPs are usually biallelic and can be encoded by $\{0, 1, 2\}$, with 0 denoting a combination of two major (i.e., common) alleles, 2 a combination of two minor alleles, and 1 a combination of a major and a minor allele (which is also referred to as a heterozygous SNP). Single nucleotide variants (SNVs) are single nucleotide positions in the genomic DNA at which different sequence alternative exists [18].

Recombination Rate (RR). Recombination is the process of determining the frequency with which characteristics are inherited together. The RR is the probability that a transmitted haplotype constitutes a new combination of alleles different from that of either parental haplotype [14].

Genome-Wide Association Studies (GWAS). GWAS are hypothesis-free methods for identifying associations between genetic regions and traits. A typical GWAS looks for common variants in a number of individuals, both with and without a trait, using genome-wide SNP arrays [17, 39].

Algorithm 1 MIATrain [53]

Input: A generative model $\text{GM}()$, the target record t , a reference dataset R of size n , the number of synthetic test sets n_s of size m , and the number k of shadow models.

Output: $\text{MIA}_t()$

```

1: for  $i = 1, \dots, k$  do
2:    $R_i \sim R^n$ 
3:    $f_i \sim \text{GM}(R_i)$ 
4:   for  $j = 1, \dots, n_s$  do
5:      $S_j^m \sim f_i$ 
6:      $S_{\text{train}} \cup S_j^m$ 
7:      $l_{\text{train}} \cup 0$ 
8:    $R'_i \leftarrow R_i \cup t$ 
9:    $f'_i \sim \text{GM}(R'_i)$ 
10:  for  $j = 1, \dots, n_s$  do
11:     $S_j^m \sim f'_i$ 
12:     $S_{\text{train}} \cup S_j^m$ 
13:     $l_{\text{train}} \cup 1$ 
14:  $\text{MIA}_t() \leftarrow \text{Classifier}(S_{\text{train}}, l_{\text{train}})$ 

```

Algorithm 2 MIAGain [53]

Input: A generative model $\text{GM}()$, the target record t , the target training set R_{out}^t of size n , the size m of the synthetic dataset, the number n_s of synthetic test sets, a reference dataset R^a , the number k of shadow models.

Output: PG_t

```

1:  $f_{\text{out}} \sim \text{GM}(R_{\text{out}}^t)$ 
2: for  $i = 1, \dots, n_s$  do
3:    $S_i \sim f_{\text{out}}^m$ 
4:    $S_{\text{test}} \cup S_i$ 
5:    $R_{\text{in}}^t \leftarrow R_{\text{out}}^t \cup t$ 
6:    $f_{\text{in}} \sim \text{GM}(R_{\text{in}}^t)$ 
7:   for  $i = 1, \dots, n_s$  do
8:      $S_i \sim f_{\text{in}}^m$ 
9:      $S_{\text{test}} \cup S_i$ 
10:   $\text{MIA}_t() \leftarrow \text{MIATrain}(\text{GM}(), t, R^a, n, m, n_s, k)$ 
11:   $\overline{\text{MIA}}_t(S_{\text{test}}) = \sum_{S_i \in S_{\text{test}}} \frac{\Pr[\text{MIA}_t(S_i) = 1]}{2 * n_s}$ 
12:   $PG_t \leftarrow (1 - \overline{\text{MIA}}_t(S_{\text{test}})) / 2$ 

```

2.2 Membership Inference Attacks

A well-understood privacy threat in genomics is determining whether the data of a target individual is part of an aggregate genomic dataset, or mixture. This is known as a *membership inference attack* (MIA) [30, 58, 64]. The ability to infer the presence of an individual’s data in a dataset constitutes an inherent privacy leak whenever the dataset has some sensitive attributes. For instance, if a mixture includes DNA from patients with a specific disease, learning that a particular person is part of that mixture exposes their health status. Overall, genomic data contains some of the most sensitive information about a person’s past, present, and future; therefore, MIAs against genomic data prompt severe privacy threats, including denial of life or health insurance, revealing predisposition to diseases and conditions, ancestry, etc.

MIAs have also been studied in the context of machine learning, aiming to infer whether a target data point was used to train a target model or not. This has been done both for discriminative [11, 45, 47, 49] and generative models [11, 24, 26]. Inferring training set membership might yield serious privacy violations. For instance, if a model for drug dose prediction is trained using data from patients with a certain disease, or synthetic health images are produced by a generative model trained on patients’ images, learning that data of a particular individual was part of the training set leaks information about that person’s health. Overall, MIAs are also used as signals that access to a target model is “leaky,” and can be a gateway to additional attacks [15].

Recently, Stadler et al. [53] present a comprehensive evaluation of MIAs in the context of synthetic data, showing that even access to a single synthetic dataset output by the target model can lead to serious privacy leakage. In our evaluation, we adapt their attacks to the context of genomic data and rely on their “Privacy Gain” metric (presented next) to quantify the difference in privacy leakage when releasing a synthetic dataset instead of the real one.

2.3 Privacy Gain (PG) from Synthetic Data Release

As our main privacy evaluation metric, we use the *Privacy Gain (PG)* [53]. The PG quantifies the privacy advantage obtained by a target t , vis-à-vis an MIA adversary, when a synthetic dataset is published as opposed to the raw data.

MIA Training. As depicted in Algorithm 1, the adversary is trained as follows. First, we take a reference dataset (which may or may not overlap with the raw data used to generate the synthetic dataset) and use it to generate a synthetic dataset (lines 1–6). This dataset is labeled as 0, i.e., it does not include the target record (line 7). The target record is then added to the dataset (line 8), and synthetic data is generated from the new dataset which includes the target record; this dataset is labeled as 1 (lines 10–13). These models are referred to as *generative shadow* models. Finally, the adversary uses the synthetic datasets to train a classifier (line 14), which distinguishes whether or not the target was used in the training of a generative model.

PG Estimation. To estimate the PG for a fixed target record and input dataset, we use Algorithm 2. First, the algorithm takes the target training set and generates n_s synthetic datasets without the target record (lines 1–4). Then, the target record is added to the training set and n_s of synthetic datasets are generated from this dataset (lines 5–9). Then, the adversary trains their attack model MIATrain (line 10). Finally, the PG for a target t is computed as $PG_t = \frac{1 - \overline{\text{MIA}}_t(S_{\text{test}})}{2}$, where $\overline{\text{MIA}}_t(S_{\text{test}}) = \sum_{S_i \in S_{\text{test}}} \frac{\Pr[\text{MIA}_t(S_i) = 1]}{2 * n_s}$ (lines 11–12).

Put simply, the PG is quantified as the difference between the probability that an attacker correctly identifies that the target record belongs to the real dataset (which is equal to 1 in this case) and the probability that the attacker correctly identifies that the target record was used in training a generative model that outputs a synthetic dataset.

PG Values. The PG ranges between 0, when publishing the synthetic dataset leads to the same privacy loss as publishing the real dataset (i.e., $\overline{MIA}_t(S_{test}) = 1$) and 0.5, when publishing the synthetic dataset perfectly protects the target from MIA (i.e., $\overline{MIA}_t(S_{test}) = 0$). This means that $PG = 0.25$ when the probability of the adversary inferring whether or not a target is part of the training set used to generate the synthetic dataset is the same as random guessing (i.e., $\overline{MIA}_t(S_{test}) = 0.5$).

Dimensionality Reduction. To reduce the effects of high-dimensionality, the MIA attacker first maps the synthetic data to a lower feature space. This allows to more easily detect the influence of the target record on the training dataset. We experiment with four different feature sets, as done in [53]: namely, a *naive* feature set, which encodes the number of distinct categories plus the most and least frequent category for each attribute, a *histogram*, which computes the frequency counts for each attribute, a *correlation*, which encodes pairwise correlations between attributes, and an *ensemble* feature set, which combines all the previously mentioned feature sets.

2.4 Datasets

In our evaluation, we use data from two projects: HapMap [38] and the 1000 Genome Project [4]. More specifically, we use 1,000 SNPs from chromosome 13 from the following three datasets:

1. *CEU Population (HapMap)*. Samples from 117 Utah residents with Northern and Western European ancestry, released in phase 2 of the HapMap project.
2. *CHB Population (HapMap)*. Samples from 120 Han Chinese individuals from Beijing, China.
3. *1,000 Genomes*. Samples from 2,504 individuals from 26 different populations released from phase 3 of the 1000 Genomes project.

3 Synthetic Data Approaches in Genomics

The ability to effectively train statistical models [7] from genomic data is very important in many applications. As many models suffer from the “curse of dimensionality” [5], i.e., models do not usually perform well on small datasets with high dimensionality, statistical and generative models have been proposed not only to mitigate possible privacy concerns of sharing genomic data but also to help “inflate” the size of the datasets for more meaningful analysis.

In this section, we provide an overview of the state-of-the-art models for generating synthetic genomic data. In particular, we discuss the Recombination model proposed by Samani et al. [48], the RBM and GAN models proposed by Yelmen et al. [61], and the WGAN model from Killoran et al. [33]. We also introduce and consider two other “hybrid” models.

Recombination Model (Recomb). Samani et al. [48] propose the use of a *recombination model* as an inference method for quantifying individuals’ genomic privacy. This is a statistical model, based on high-order SNV correlation that relates linkage disequilibrium patterns to the underlying recombination rate. Given a set of sampled haplotypes, the model relates their distribution to the underlying recombination rate.

Also, [48] shows how to use this method to generate synthetic samples in order to perform Principal Component Analysis (PCA). The recombination model yields a distribution closer to the real data than models using only linkage disequilibrium and allele frequencies. In order to obtain the underlying recombination rate, the model uses a “genetic map,” which includes the recombination rate. This is provided with the dataset for the HapMap datasets, but not for the 1000 genomes data. For the latter, we use the scripts from [2].

Restricted Boltzmann Machines (RBMs). RBMs [52] are generative models geared to learn a probability distribution over a set of inputs. RBMs are shallow, two-layer neural nets: the first layer is known as the “visible” (on input) layer and the second as the hidden layer. The two layers are connected via a bipartite graph – i.e., every node in the visible layer is connected to every node in the hidden one, but no two nodes in the same group are connected to each other, allowing for more efficient training algorithms. The learning procedure consists of maximizing the likelihood function over the visible variables of the model. The RBM models re-create data in an unsupervised manner through many forward and backward passes between the two layers, corresponding to sampling from the learned distribution. The output of the hidden layer passes through an activation function, which then becomes the input for the hidden layer. RBMs are typically used for dimensionality reduction, classification, regression, collaborative filtering, topic modeling, etc.

As mentioned earlier, Yelmen et al. [61] use RBMs to generate synthetic genomic data. In our evaluation, we follow the same RBM settings as [61]. More specifically, we use a ReLu activation function, with the visible layer having the same size

as the input we considered (1,000 features) and with the number of hidden nodes set to 100. The learning rate is set to 0.01, the batch size to 32, and we iterate over 2,000 epochs.

Generative Adversarial Networks (GANs). A GAN is an unsupervised deep learning model consisting of two neural networks, a generator and a discriminator, which compete against each other in the form of a game setting. During training, the generator’s goal is to produce synthetic data and the discriminator evaluates them against real data samples in order to distinguish the synthetic from the real samples. The training objective is to learn the data distribution so that the data samples produced by the generator cannot be distinguished from real data by the discriminator.

Again, we use the GAN approach proposed by Yelmen et al. [61], mirroring their experimental settings. More precisely, the generator model consists of an input layer with latent dimension set to 600, and two hidden layers, of sizes 512 and 1,024 respectively. The discriminator consists of an input layer with size equal to the number of SNPs evaluated (1,000), and two hidden layers of sizes 512 and 256 respectively, as well as an output layer of size 1. The output layer for the generator uses \tanh as an activation function and the output layer for the discriminator uses the sigmoid activation function. For both the generator and discriminator, we compile them using the Adam optimization and binary cross-entropy as the loss function.

Recombination RBM (Rec-RBM). To overcome issues caused by low numbers of training samples, we propose a hybrid approach between the Recomb and the RBM models. In other words, we use the former to generate extra samples, which we then use, together with the real data samples, to train the RBM model with the same parameters as before. We do so to explore whether having more data points available to train the model improves the utility of the synthetic data.

Recombination GAN (Rec-GAN). Similar to Rec-RBM, we use the Recomb model to generate extra training samples for the GAN model, using the same parameters as before. Again, we want to study whether having a larger dataset available for training the GAN improves the overall utility of the synthetic data output by it.

Wasserstein GAN (WGAN). Killoran et al. [33] propose an alternative GAN model by treating DNA sequences as a hybrid between natural language and computer vision data. The sequences are one-hot encoded, the GAN is based on a WGAN architecture trained with a gradient penalty [22], and both the generator and discriminator use convolutional neural networks [34] and a residual architecture [25], which includes skip connections that jump over some layers. The authors also propose a joint method combining the GAN model with an activation maximization design [37, 51, 63] in order to tune the sequences to have desired properties. We do not, however, include the joint model in our evaluation, as we focus on a range of statistics as opposed to a single desired property.

In our evaluation, we use the WGAN model with the default parameters from the implementation in [1]. The generator consists of an input layer with dimension of the latent space set to 100, followed by a hidden layer with size 100 times the length of the sequence (1,000), which is then reshaped to (length of the sequence, 100), followed by 5 resblocks. Finally, there is a 1-D convolutional layer followed by the output layer, which uses softmax. The discriminator has a very similar architecture but in a different order – i.e., it starts with the input layer to which the one-hot sequences are fed, that is followed by the 1-D convolutional layer, then the 5 resblocks, followed by the reshape layer and the output layer of size 1. We perform 5 discriminator updates for every generator update. Both the generator and discriminator use Adam optimization and their learning rates are set to 0.0001, while the loss as mentioned is adjusted by a gradient penalty. We use a batch size of 64. In our experiments, the WGAN model converges after about 80 iterations; so, as opposed to the 100,000 proposed by the authors, we train the model for 100 iterations in our evaluation.

4 Utility Evaluation

We now perform a comprehensive utility evaluation of the synthetic data generated by the models presented in Section 3. We look at common summary statistics used in genome-wide association studies, aiming to assess the accuracy loss due to the use of synthetic datasets. More specifically, we analyze how well data generated by the generative models preserves allele frequencies, population statistics, and linkage disequilibrium, and how close the distribution of the synthetic data is to the real data for principal component analysis.

4.1 Allele Statistics

Major Allele Frequency (MAF). In population genetics, the *major allele frequency* (MAF) is routinely used to provide helpful information to differentiate between common and rare variants in the population, as it quantifies the frequency at which the most common allele occurs in a given population. We start our utility analysis by comparing MAFs in the synthetic data vs. the real data.

In Figure 1, we plot the MAF at each position for the real datasets and for the synthetic samples, over the CEU and CHB populations, and the 1000 Genomes dataset. For CEU/CHB (Figure 1a–1b), we observe that Recomb and WGAN replicate best the allele frequencies in the real data. On the other hand, GAN and Rec-GAN fail to do so, and in fact, the generated

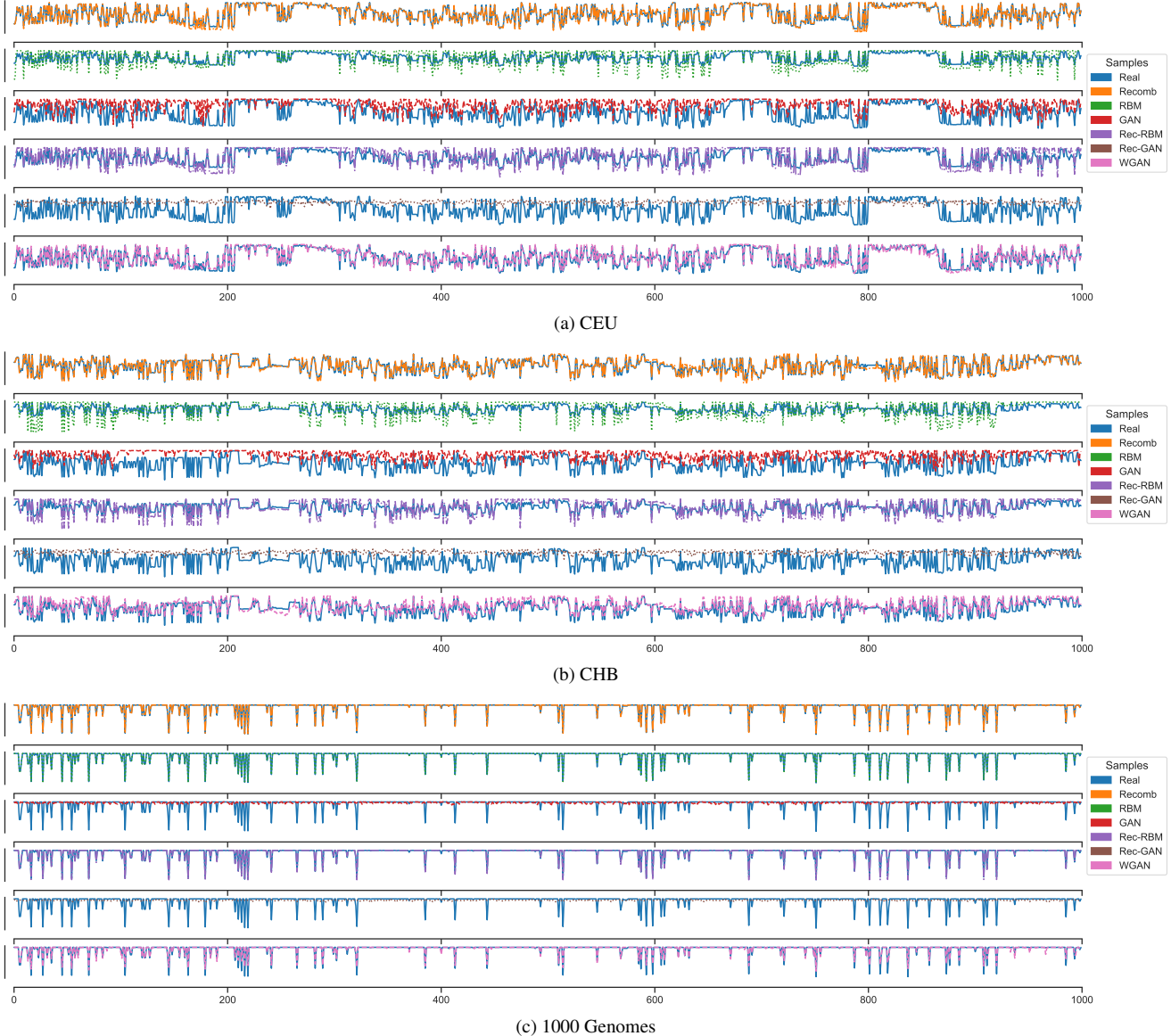


Figure 1: Major allele frequencies for synthetic data generated by the models, plotted against the real data, for the CEU population, the CHB population, and the 1000 Genomes dataset.

samples seem random. The RBM model, even though not as close to the real frequencies as Recomb, performs better than the GAN and Rec-GAN models. In fact, RBM further improves when combined with Recomb (see Rec-RBM).

For 1000 Genomes (Figure 1c), Recomb’s MAF distribution is also similar to the real data’s. However, RBM and Rec-RBM both display MAFs close to the real data, whereas, even with more training samples available, the GAN and Rec-GAN models still seem to produce random results. Moreover, WGAN does not match the MAF distribution for this population as closely. Overall, the difference in the MAF distributions across datasets is likely to be due to fewer samples available for the HapMap populations compared to the 1000 Genomes.

Alternate Allele Correlation (AAC). To evaluate whether the real and synthetic data are *genetically* different, in Figure 2, we plot the *alternate allele correlation* (AAC). The more similar two populations are, the closer the SNPs should be to the diagonal, as in the leftmost plots, where we have the real data against itself. The strongest AAC is with the synthetic data generated by Recomb. On the opposite side of the spectrum, the synthetic data generated by GAN and Rec-GAN have weak correlations. For the CEU and CHB populations, we find Rec-RBM to yield stronger AACs than simple RBM and the WGAN. For the 1000 genomes dataset (Figure 2c), there is a strong correlation between the alternate alleles for the real data and Recomb, RBM, Rec-RBM, and WGAN.

Site Frequency Spectrum (SFS). Another summary statistic that captures essential information about the underlying distri-

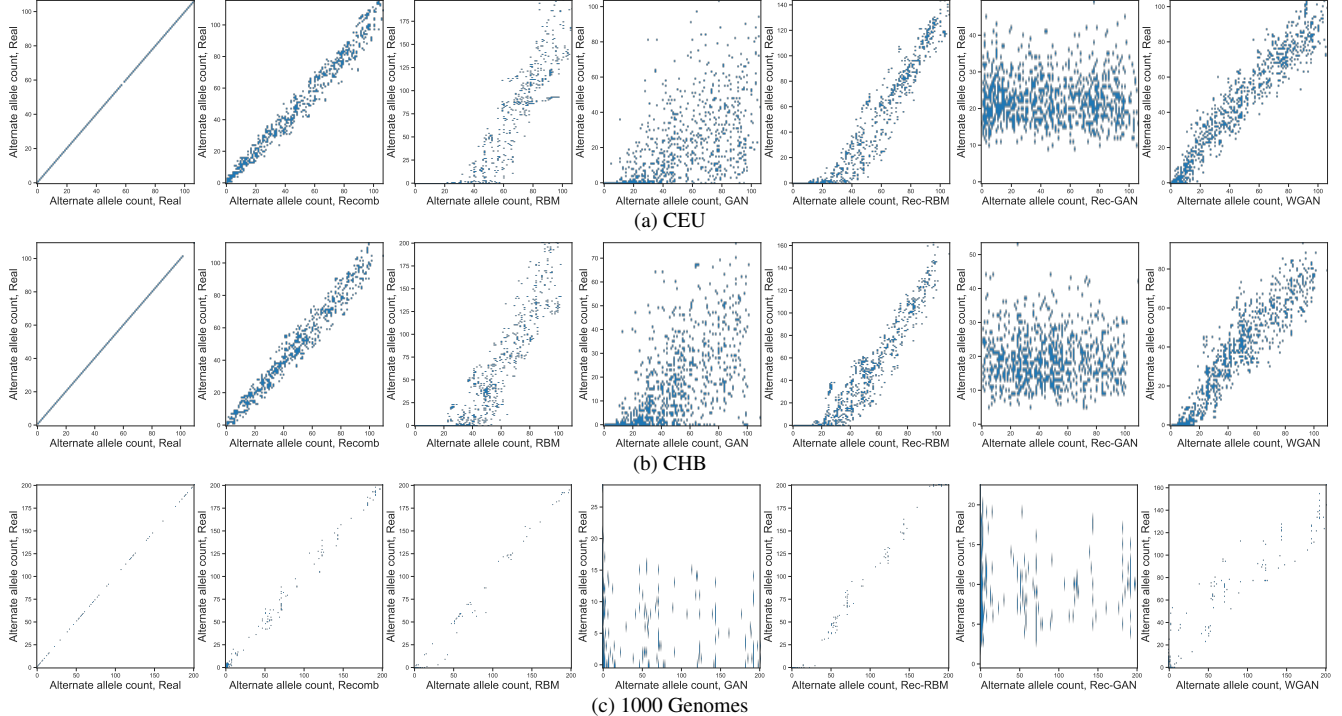


Figure 2: Alternate allele correlation for the CEU population, the CHB population, and the 1000 Genomes dataset.

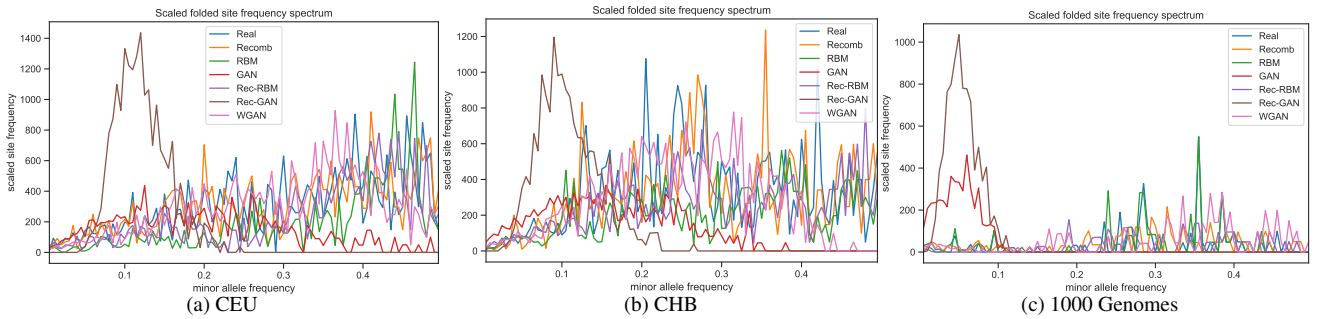


Figure 3: Frequency spectrum analysis for the CEU population, the CHB population, and the 1000 Genomes dataset.

bution of the allele frequencies of a given set of SNPs in a population or sample is the SFS [19, 20]. Basically, it provides a histogram whose size depends on the number of sequenced individuals. In Figure 3, we plot the scaled folded SFS, which is the distribution of counts of minor alleles in a sample calculated over all segregating sites. We scale this value so that a constant value is expected across the spectrum for neutral variation and constant population size, which yields the best visual comparisons. If the distribution of allele frequencies for the synthetic samples matches that for the real data, we would expect to see the two spectra aligned.

With the HapMap populations (Figure 3a–3b), Rec-GAN suggests an excess of rare variants for a minor allele frequency around 0.1. Whereas GAN seems to generate data closer to a neutral expectation, i.e., the synthetic dataset describes a more stable population. Similarly, for the 1000 Genomes (Figure 3c), Rec-GAN has an excess of rare variants for a minor allele frequency less than 0.1, and this is also displayed, at a lower scale, by the GAN-generated data.

We also compute the Kolmogorov-Smirnov (KS) two-sample test [27] for the goodness of fit on the SFS for each dataset vs. the synthetic data (see Table 1). The test compares the agreement between the cumulative distributions of two independent samples. For every two-samples test, the 95% critical value is approximately 0.195 (as we have 100 samples in each dataset), so we can reject the null hypothesis (that there is no difference between the distributions) for all synthetic data above this value. For both CEU and CHB, we cannot reject the null hypothesis only for the samples generated by the Recomb and the WGAN models. For the 1000 Genomes dataset, we reject the null hypothesis for synthetic data generated by the GAN and Rec-GAN.

Models	SFS						% Heterozygous Samples					
	CEU		CHB		1000 Genomes		CEU		CHB		1000 Genomes	
	D	p-value	D	p-value	D	p-value	D	p-value	D	p-value	D	p-value
Recomb	0.07	0.89	0.07	0.89	0.18	<0.1	0.19	0.47	0.29	<0.001	0.32	<0.001
RBM	0.34	<0.001	0.28	<0.001	0.12	0.44	0.64	<0.001	0.70	<0.001	0.13	0.34
GAN	0.40	<0.001	0.41	<0.001	0.23	<0.01	0.90	<0.001	1.00	<0.001	0.57	<0.001
Rec-RBM	0.26	<0.01	0.23	<0.01	0.06	0.99	0.99	<0.001	1.00	<0.001	0.40	<0.001
Rec-GAN	0.64	<0.001	0.58	<0.001	0.25	<0.01	0.55	<0.001	0.68	<0.001	0.52	<0.001
WGAN	0.09	0.79	0.18	<0.1	0.19	<0.1	0.17	<0.1	0.39	<0.001	0.45	<0.001

Table 1: Two-sample (real vs. synthetic data) Kolmogorov-Smirnov test performed on the SFS and the percentage of heterozygous samples.

4.2 Population Statistics

Next, we look at population statistics to determine how close to the real dataset is the synthetic data. In particular, we look at the percentage of heterozygous variants for both real and synthetic samples, at the fixation index, and at the Euclidean Genetic Distance.

Heterozygosity. The condition of having two different alleles at a locus is denoted as heterozygosity. The percentage of heterozygous variants is commonly used in population studies, as a low percentage of heterozygous variants implies less diversity in the population. In Figure 4a–4b, we plot the percentage of heterozygous variants in each sample for the CEU/CHB populations, comparing the real statistics (blue/leftmost bars) vs. those computed on the synthetic data. In both cases, Recomb and WGAN yield similar percentages to the real dataset. Whereas, with GAN and RBM, the percentage decreases, suggesting that both models produce more homozygous variants. Moreover, even though for the major allele frequencies Rec-RBM produces variants with statistics closer to the real data, the percentage of heterozygous variants turns out to be the lowest for both populations. By contrast, Rec-GAN produces a higher percentage of heterozygous variants than GAN, even though the major allele frequencies are not aligned with the original samples.

With the 1000 Genomes (Figure 4c), the percentage of heterozygous samples in the real data is lower across all samples. Once again, and in line with previous results, GAN and the Rec-GAN significantly deviate from the percentages of heterozygous samples found in the real data.

We also run a Kolmogorov-Smirnov (KS) two-sample test [27] for the goodness of fit on the percentage of heterozygous samples for each dataset vs. the synthetic data (see Table 1). Interestingly, for both Recomb and WGAN, we do not reject the null hypothesis for the CEU dataset, but we do for the CHB dataset. In fact, for all of the models trained on the CHB dataset, we reject the null hypothesis. For the 1000 Genomes dataset, we do not reject the null hypothesis only for RBM.

Fixation Index (F_{ST}). Another way to assess how *different* are groups of populations from each other is to use the fixation index [28]. This provides a comparison of differences in allele frequency, with values ranging from 0 (not different) to 1 (completely different/no alleles in common). In Figure 5, we compare the fixation index values for the real data against the synthetic samples. For illustration purposes, we also include F_{ST} of the real data against itself, which obviously yields $F_{ST} = 0$.

Recomb is once again the closest to the real data, which confirms the alignment from Figure 1. The F_{ST} value for the synthetic data produced by RBM is, for both CEU and CHB populations, less than 0.10, however, the hybrid Rec-RBM model further reduces this value to less than 0.04, and so does WGAN. For both populations, data generated by GAN and Rec-GAN has the highest F_{ST} , although, for the CHB population, the latter increases it and for the CEU population reduces it. Finally, for the 1000 genomes, Recomb, RBM, and Rec-RBM all have F_{ST} close to the real data. While still having a low F_{ST} , WGAN has a slightly higher value. Whereas, with GAN and Rec-GAN, F_{ST} significantly deviates from the real data, even with the increased number of samples of this dataset.

Euclidean Genetic Distance (EGD). Since the fixation index does not easily allow for pairwise comparisons among populations, in Figure 6, we plot the Euclidean Genetic Distance (EGD) between the samples in each dataset. EGD is routinely used as a measure of divergence between populations, and shows the number of differences, or mutations, between two populations; a distance of 0 means that is no difference in the results, i.e., there is an exact match. From Fig. 6a–6b, where the EGD on the diagonal is 0, we observe that, for both CEU and CHB populations, the synthetic samples generated by GAN are closer to each other than by the other models. Rec-GAN generates samples with EGD close to 0, suggesting that there are very few differences between them, as well as samples with a distance of around 30. As for the other population statistics, Recomb generates samples that match the differences observed in the real data the closest, for both populations. For RBM, the samples generated have fewer differences than the real data. Perhaps more interestingly, Rec-RBM yields samples with a higher divergence than the real data; this can be a consequence of the low percentage of heterozygous samples found in the synthetic samples generated by this model (recall Figure 4). The samples from WGAN match some of the differences

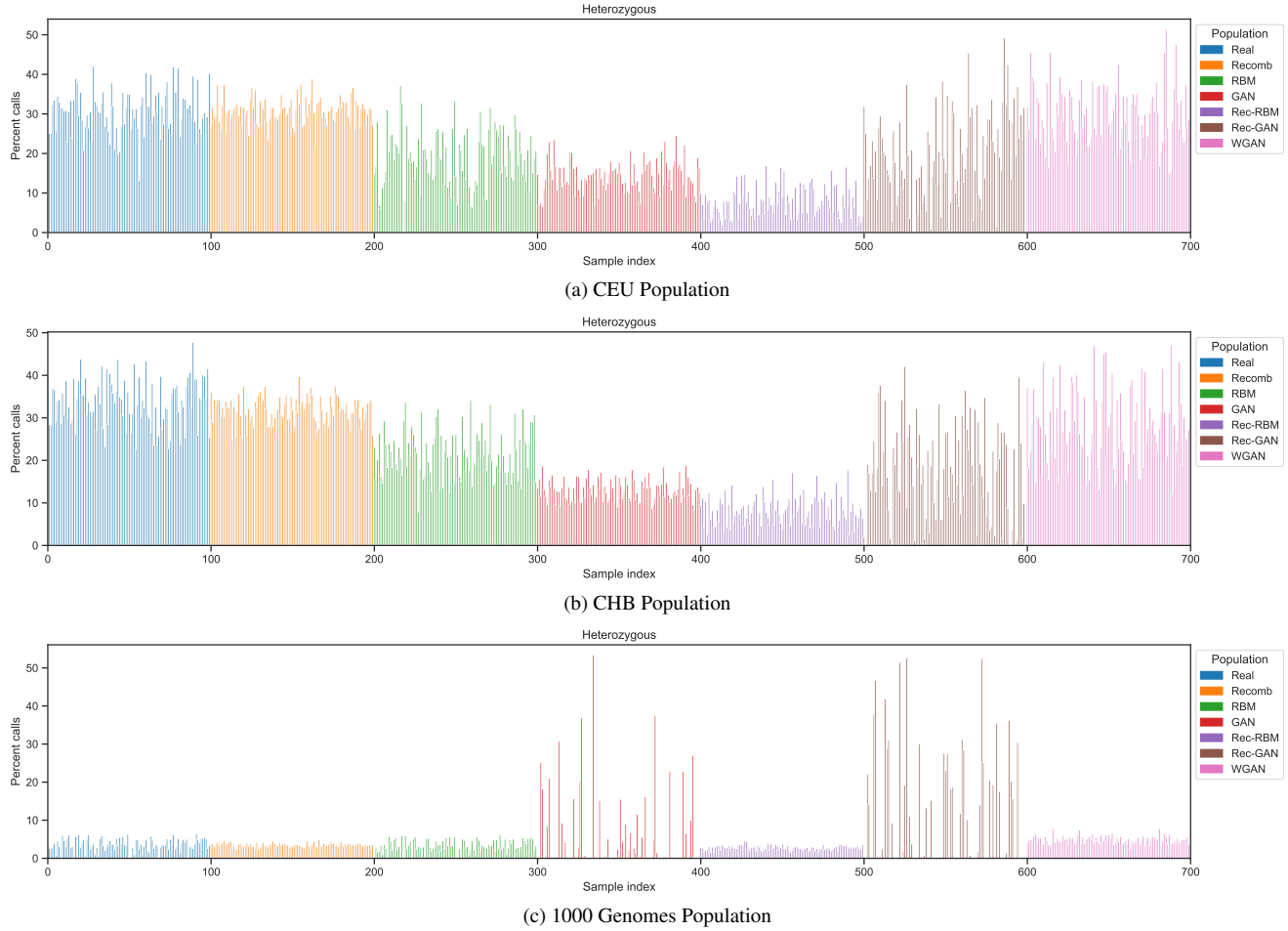


Figure 4: Percentage of heterozygous variants in each sample in the dataset for CEU, CHB populations, and the 1000 Genomes dataset.

observed in the real data, but the model also yields a few samples with a higher divergence.

Finally, for the 1000 Genomes (Figure 6c), we find that all samples in the real data have closer EGDs between each other. In fact, the samples generated by RBM yield a similar pattern in the EGD distances. Although Recomb, Rec-RBM, and WGAN do too, they exhibit a lower distance, on average, between samples. As for CEU/CHB populations, GAN and Rec-GAN models overall fail to capture the differences between samples.

4.3 Linkage Disequilibrium (LD) Analysis

Linkage disequilibrium (LD) captures the non-random association of alleles at two or more positions in a general population – i.e., those alleles do not occur randomly with respect to each other. In Genome-Wide Association Studies, LD allows researchers to optimize genetic studies, e.g., by preventing genotyping SNPs that provide redundant information [10]. In Figure 7, we plot the r^2 value for LD based on the Rogers-Huff method [44]. This ranges from 0 (there is no LD between the 2 SNPs) to 1 (the SNPs are in complete LD, i.e., the two SNPs have not been separated by recombination and have the same allele frequencies).

For CEU and CHB populations, RBM generates samples that display a stronger LD than the real data. With more training samples, Rec-RBM yields a weaker LD, but still stronger than the real data for both models. On the other side of the spectrum, for Rec-GAN, the LD for the synthetic data is the weakest. For the 1000 Genomes, we find a stronger LD between the real samples than with the other two datasets. RBM generates samples that are almost indistinguishable from the real data in terms of LD. The LD in the synthetic datasets generated by Recomb, Rec-RBM, and WGAN have lower correlations than RBM, with GAN and Rec-GAN both failing to preserve the LD.

4.4 Principal Component Analysis (PCA)

Finally, we further study the difference between synthetic and real data by performing a principal component analysis on the corresponding samples. We extract the first two principal components and project the real and synthetic datasets on these two

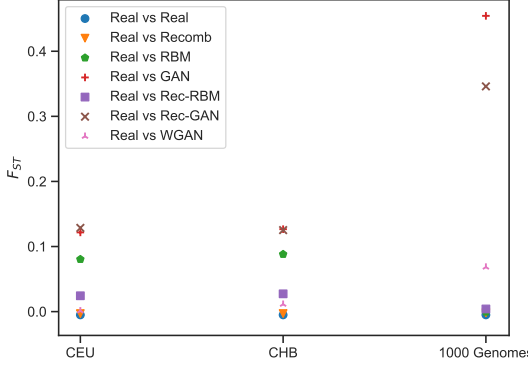


Figure 5: Fixation index values for the CEU and CHB populations, and the 1000 Genomes dataset.

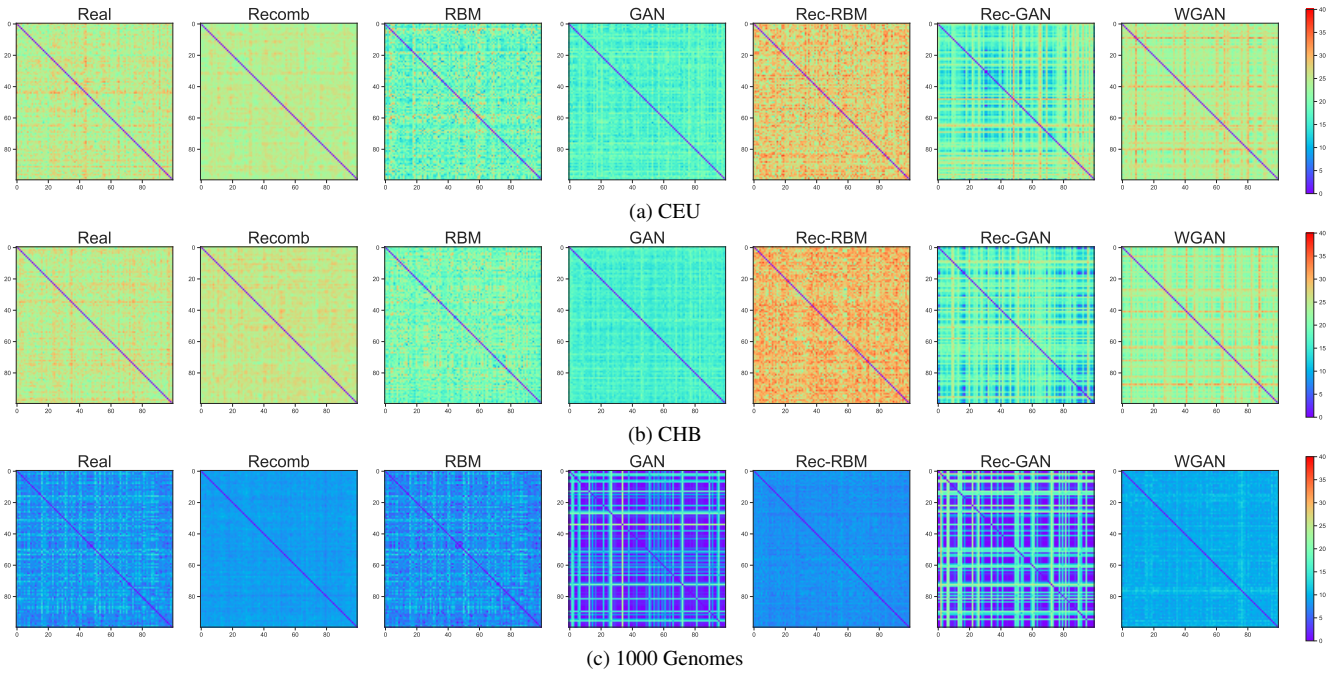


Figure 6: Pairwise Euclidean Genetic Distance (EGD) between individuals.

components to show how the synthetic samples are distributed, compared to the real data.

Figure 8 presents this 2D visualization. For both HapMap populations, Recomb has a close distribution to the real data, which, according to [48], is due to the fact that the genetic recombination model considers all the correlations between SNPs and builds a higher-order model. For the 1000 Genomes, once again, the GAN and Rec-GAN models perform quite poorly, generating samples with a different distribution than the real samples. In contrast to the HapMap populations, the samples from Recomb are all centered around 0 and fail to simulate the distribution given by the real data, and similar results are in the case of samples generated by Rec-RBM.

4.5 Take-Aways

Our utility evaluation shows that, while generative machine learning models perform well in synthesizing image data, there is still a need for progress when it comes to genomic data. Overall, the Recomb model, which is based on high-order SNV correlations, generates synthetic data preserving most statistical properties displayed by the real data, even when few samples are available. We get better utility when the genetic map is included with the data, rather than generated from the existing data. With RBM, more training samples improve the quality of the synthetic data, as evidenced by the difference between the HapMap populations and the 1000 Genomes dataset.

We also find that, when few samples are available for training, the hybrid Rec-RBM model approach helps improve the quality of samples compared to just RBM. This is clear from the utility of the synthetic data on the two smaller HapMap datasets. For the 1000 genomes, it is not surprising that the performance of Rec-RBM is worse compared to RBM since Re-

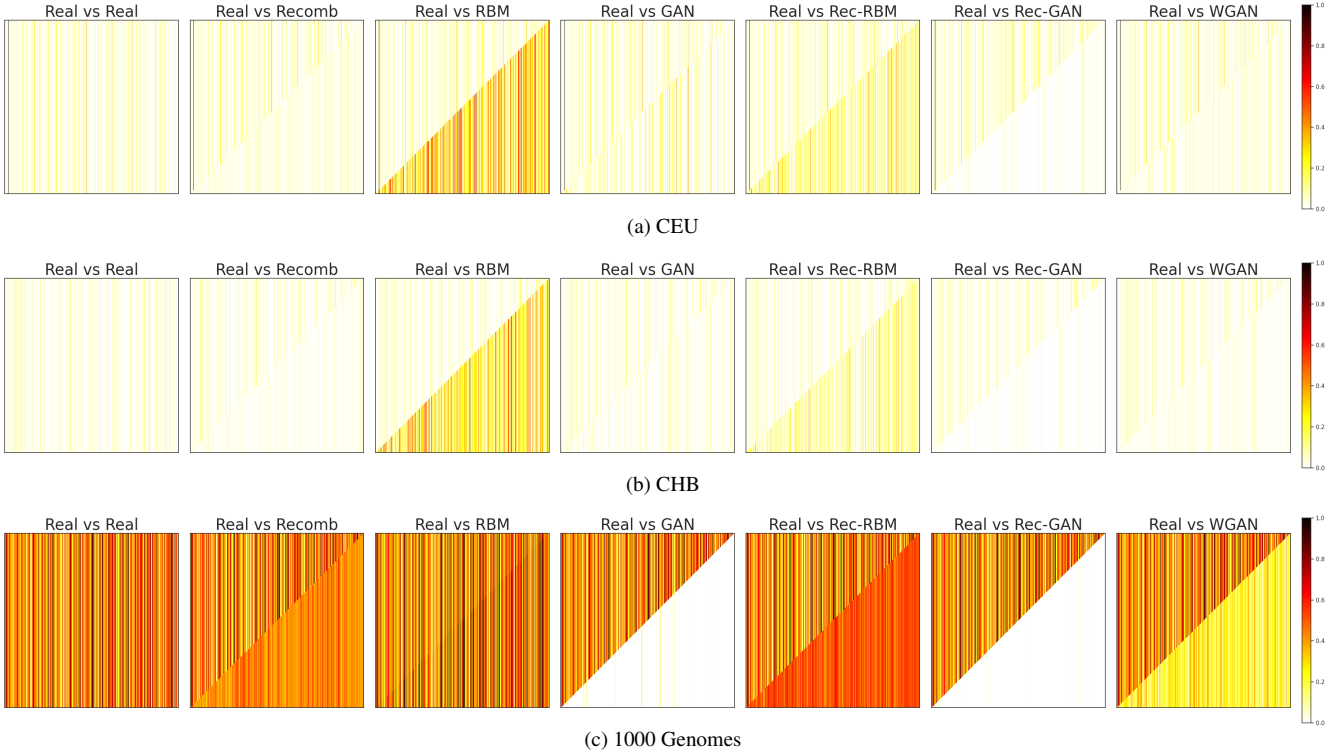


Figure 7: Pairwise Linkage Disequilibrium for Real vs. Synthetic Samples.

comb does not generate as “useful” samples as for the other two datasets. Finally, the GAN and the Rec-GAN models generate samples with the lowest utility, regardless of the number of samples available for training. However, the data generated by WGAN preserves most statistical properties of the real data.

5 Privacy Evaluation

Next, we evaluate the vulnerability of the synthetic data to Membership Inference Attacks (MIAs). To do so, we measure the Privacy Gain PG (see Section 2.3) obtained by releasing a synthetic dataset instead of the real data. Recall that, if the synthetic data does not hide nor give any additional information to an MIA attacker, PG_t , for a target record t , should have a value of around 0.25.

We present experiments for both a “standard” MIA and a novel attack, which we denote as MIA with *partial information*. The latter essentially assumes that the adversary only has access to partial data from the target sequence. We exclude GAN and Rec-GAN from the evaluation since they yield poor utility performance, so there is not really any point in evaluating their privacy.

Throughout our evaluation, we randomly choose 10 targets from each dataset across 10 test runs. In each run, we fix the target and sample a new training cohort. We train the attack classifier using 5 shadow models, using 100 synthetic training sets for each of them. We then evaluate the privacy gain on 100 synthetic datasets, with a split of 50 sets generated from a training set including the target, and 50 sets generated without. Finally, we report the PG for each test and each target as the average PG across all synthetic datasets tested.

5.1 Privacy Gain Under Membership Inference Attack

We use three adversarial classifiers: K-Nearest Neighbor (KNN), Logistic Regression (LogReg), and Random Forest (Rand-Forest). We use four feature sets, as described in Section 2.3: Naive ($\bullet F_{\text{Naive}}$), Histogram ($\bullet F_{\text{Hist}}$), Correlations ($\bullet F_{\text{Corr}}$), and an Ensemble feature set ($\bullet F_{\text{Ens}}$).

5.1.1 HapMap Populations

In Figure 9, we report the PG value for targets randomly chosen from the two HapMap populations.

KNN. For CEU, using KNN (Figure 9a, left), we find that over 74% of the targets in the synthetic dataset generated by Recomb have a PG lower than the random baseline (0.25) for the Ensemble, Correlations, and Histogram feature sets. With

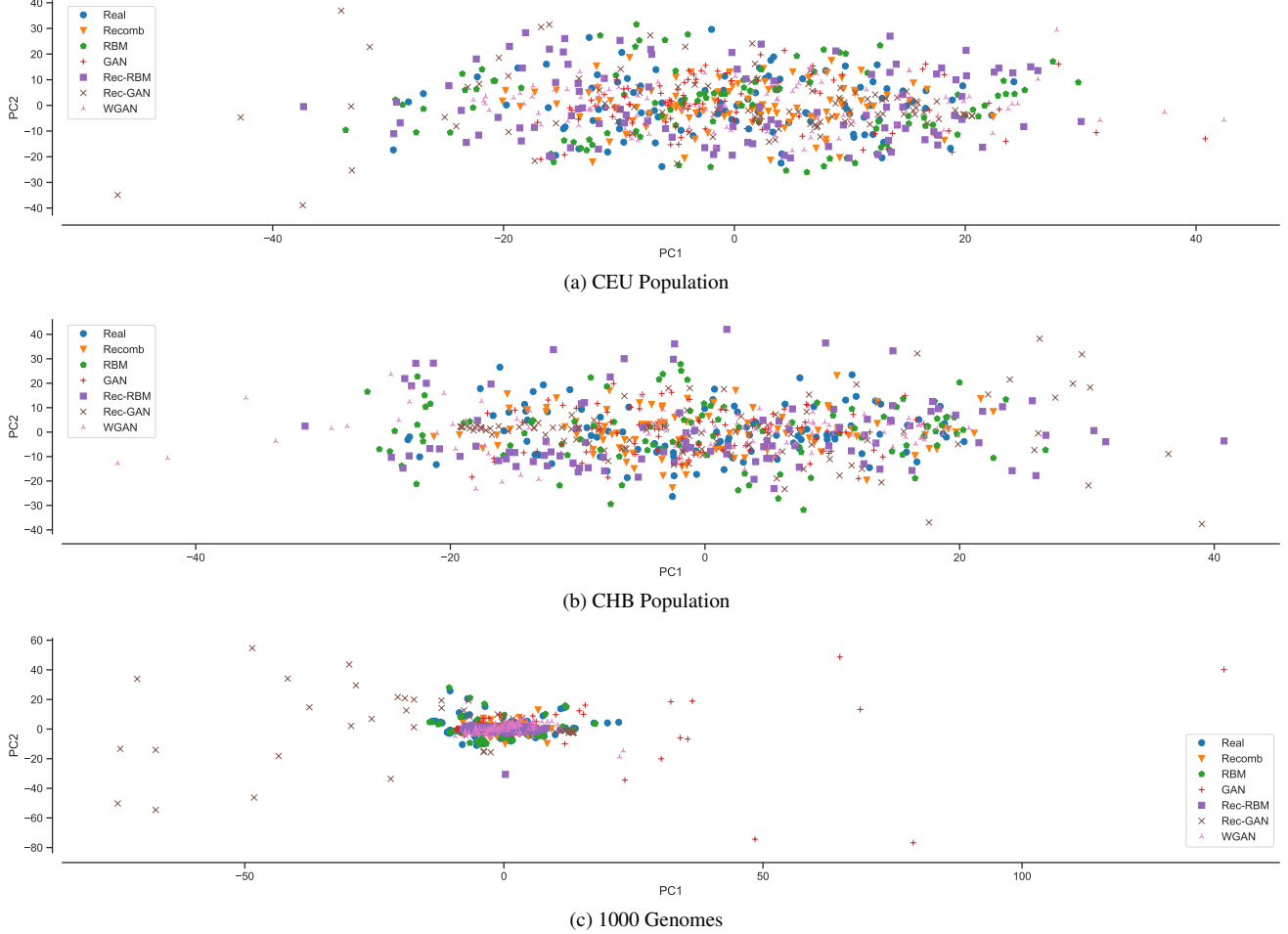


Figure 8: 2D Principal Component Analysis (PCA) visualization of the real and synthetic sequences.

RBM, there are between 84% and 88% of the targets, depending on the feature set, that have a PG of 0.25; in other words, for these targets, the probability of the adversary inferring their presence in the training set is the same as random guessing. However, between 10% and 15% of the targets have no PG at all, whereas, there are between 1% and 4% of the targets, depending on the feature set, for which the synthetic data perfectly protects the target from MIA (PG=0.5). With Rec-RBM, at least 59% of the targets have a PG of 0.25 under the four feature sets. With WGAN, at least 48% of the targets have a PG of 0.25, depending on the feature set.

For the CHB population (Figure 9b, left), we find that over 60% of the targets generated by the Recomb, with all features, have PG below the random guess baseline. With RBM, between 89% and 97% of targets have PG of exactly 0.25 across all feature sets, i.e. the synthetic dataset generated by the RBM for these targets does not hide nor give new information to the attacker about their membership to the synthetic dataset. Interestingly, for the Correlations feature set, there is no target that has PG lower than 0.25. As for the CEU population, about 50% of the targets across all feature sets have a PG of 0.25 for data from Rec-RBM, and at least 47% of targets from WGAN.

LogReg. Using LogReg, both Recomb and RBM have the lowest PG among all attack classifiers, for both HapMap populations. For CEU (Figure 9a, middle), using the Histogram feature set, 94% (resp., 96%) of the targets from Recomb (resp., RBM) have PG below 0.25, which is the random guess baseline. Under Correlations, 99% (resp., 97%) of the targets in Recomb (resp., RBM) have PG below 0.25, while, for the Ensemble feature set, 96% (resp., 98%) of the targets from Recomb (resp., RBM) have PG below 0.25. With Rec-RBM, we find that between 52% and 56% of the targets across all feature sets have PG above 0.25, and with WGAN, between 50% and 57% of the targets across all feature sets have PG above 0.25. Moreover, for the Rec-RBM and WGAN-generated data, there is no target that consistently has a lower PG than the random guess baseline across all test runs.

For CHB (Figure 9b, middle), with synthetic data generated by Recomb, the average PG is below the random baseline (0.25) for 99% of the targets in the Histogram feature set, 97% for Correlations, and for 96% for Ensemble. For RBM, 79% of the targets in the Histogram feature set have a PG below 0.25. Under the Ensemble feature set, 84% of the targets have

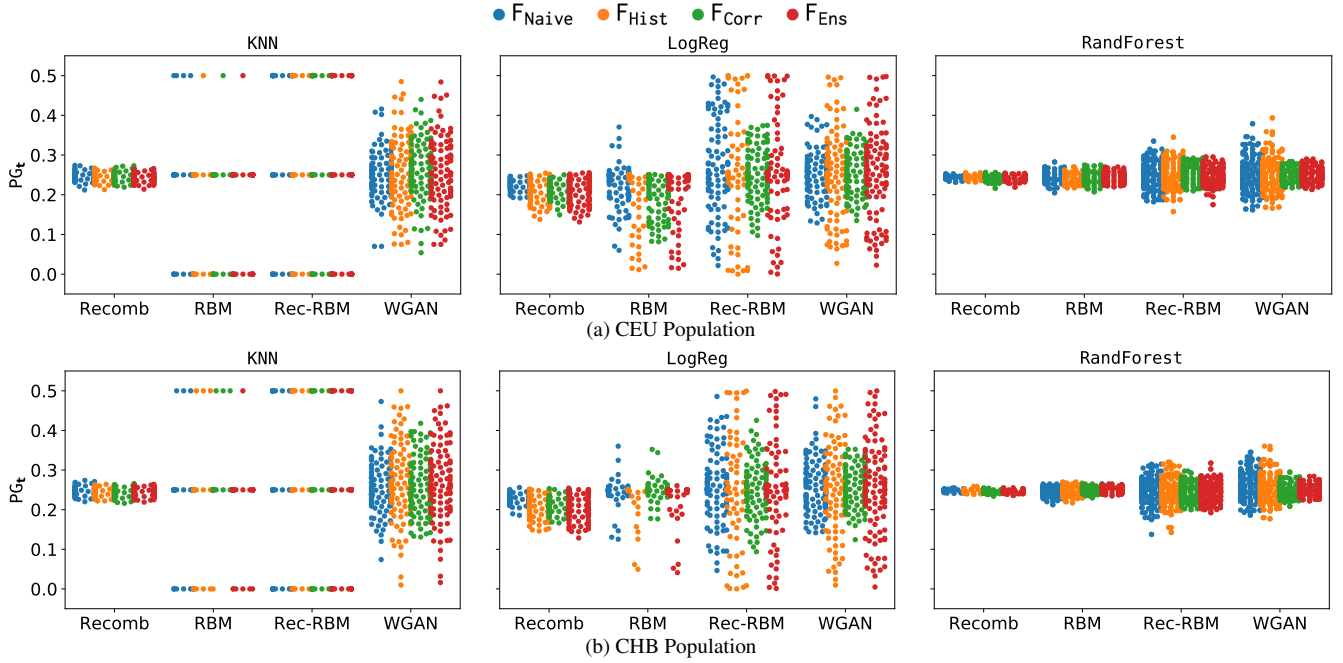


Figure 9: Privacy Gain (PG) of different models over the two HapMap populations.

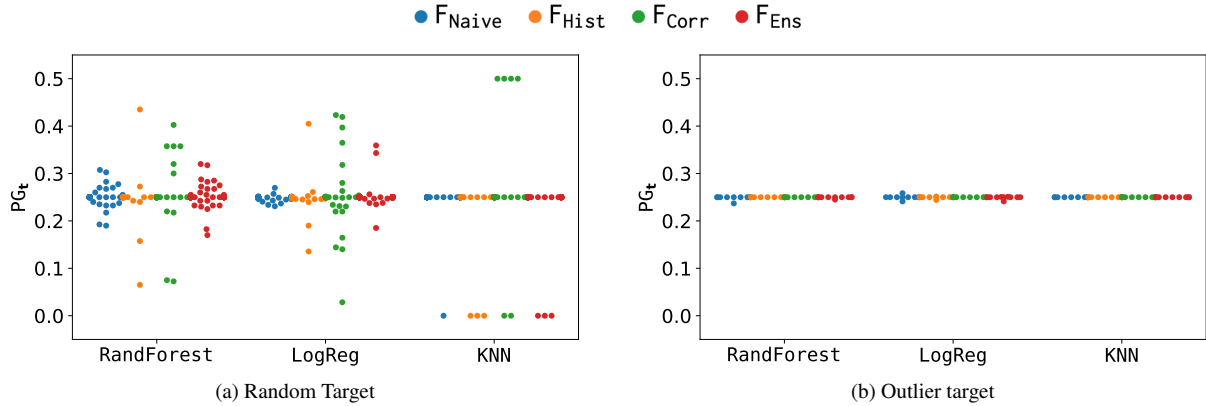


Figure 10: Privacy Gain (PG) of RBM over the 1000 Genomes dataset.

PG below 0.25. For synthetic data generated by Rec-RBM, we find that 54% of the targets from the Histogram and Ensemble feature sets have PG lower than 0.25 and 46% have PG over 0.25. For the Naive and Correlations feature sets, respectively, 45% and 47% of the targets have PG lower than the random guess baseline. For WGAN-generated data, Correlations feature set yields most targets (55%) with PG<0.25.

RandForest. When using RandForest as the attack classifier on data from the CEU population (Figure 9a, right), with RBM-generated data, 73% of the targets from both Correlation and Histogram feature sets have lower PG than the random baseline. This is for 69% and 62% of the targets with, respectively, Ensemble and Naive feature sets. For the synthetic data generated by Rec-RBM, about 51% of targets have a PG of over 0.25, and 49% of the targets have PG of less than 0.25, across all feature sets. For WGAN, between 46% and 59% of the targets from all feature sets have a PG less than the random guess baseline (0.25), with the Correlations feature set having the least percentage of vulnerable targets (59%).

For CHB (Figure 9b, right), the lowest privacy gain for the samples generated by Recomb: over 79% of all targets for each of the four feature sets have PG lower than the random baseline. For the synthetic samples from RBM, 71%, 61%, and 53% of the targets under the Naive, Histogram, respectively, Ensemble feature sets have PG lower than 0.25. However, for the Correlations feature sets, we find that 55% of the targets have a PG of 0.25, meaning that, those targets are protected from MIA. For the synthetic samples generated by Rec-RBM, 54% of the targets from the Histogram and Ensemble feature sets and 47 and 45% of the targets from the Correlations and Naive, respectively, have PG lower than 0.25. Finally, for the WGAN, we find that between 44% and 53% of the targets have PG>0.25 across all four feature sets.

5.1.2 1000 Genomes Population

For the 1000 Genomes population, we focus our analysis on the RBM model, as it generated synthetic data closest to the real data across all utility metrics evaluated.

Random Target. In Figure 10a, we plot the PG for the synthetic data generated by RBM, for randomly chosen targets. With the RandForest MIA classifier, we observe that 56%, 75%, 92%, and 50% of the targets have PG higher than the random guess baseline ($PG \geq 0.25$) for, respectively, Naive, Histogram, Correlations, and Ensemble feature sets. The high percentage of targets that have a $PG \geq 0.25$ for the Correlations suggests that the impact of a single target in the training dataset of the RBM on the correlations of the synthetic dataset is minimal.

Then, with the LogReg classifier, we find a high variation in PG, similar to the HapMap populations in the case of Rec-RBM. Under the Naive feature set, half of the targets have PG gain below the random guess baseline. Similarly, 43%, 45%, and 43% of targets have a PG lower than 0.25 for, respectively, the Correlations, Histogram, and Ensemble feature sets. Finally, for the KNN classifier, over 94% of the targets have a PG of 0.25 across all feature sets.

Outlier Target. To better understand whether, with more training data, a target’s signal in the synthetic dataset is diluted, we also test an “extreme” outlier case. That is, we craft an outlier target that has only minor alleles at all positions. While we are aware that this case would be extremely rare in a real-world scenario, our goal is to observe whether, and how much, this impacts PG. To this end, in Figure 10b, we plot the PG of this outlier case across 10 test runs.

With RandForest, we find that, under the Ensemble feature set, PG is below 0.25 for 8 of the 10 test runs. In fact, this is the only combination between attack classifier and feature set for which a greater percentage of the targets have a lower privacy gain than in the random target case. For the Naive feature set, in only 3 of the test runs, PG is below the random baseline. For the Correlations and Histogram feature sets, all test runs yield PG of 0.25 or above. With LogReg, 4 out of 10 of the test runs for the Naive, Histogram, and Correlations feature sets yield PG below 0.25. For Ensemble, this happens for 6 test runs. Finally, with KNN, across all feature sets, PG for all test runs is 0.25, i.e., the synthetic data does not disclose any membership information regarding the outlier.

While there are differences across classifiers and feature sets, the PG, for all test runs in this outlier target case, is centered around 0.25. This is evident from Figure 10b, which implies that, across all test runs, the accuracy of the MIA is not much better than random guessing.

5.1.3 Take-Aways

The different combinations of datasets, attack classifiers, and feature sets, yield varied results with respect to privacy. This is due to two main reasons: first, not all classifiers have the same accuracy on tasks for the same dataset, as shown in previous work [6]. Second, the features that the generative model preserves after training will “reflect” in the synthetic data; thus, this will impact the PG based on the feature extraction method.

On the HapMap populations, while the utility evaluation shows that Recomb-generated synthetic data is “closest” to the real data, it does so with a significant privacy loss in comparison to the other models. The RBM-generated synthetic data is the most vulnerable under the LogReg classifier, with at least 70% of the targets across both populations and all feature sets having PG below the random guess baseline. This suggests that, with few data samples available for training, the RBM model is likely to overfit and is thus susceptible to MIAs.

For Rec-RBM and WGAN, the attacker cannot reliably predict membership, i.e., the addition of extra samples from the Recomb model in the training of the Rec-RBM dilutes the target’s signal in the training data. However, for both models, we still find combinations of targets and training sets for the attack classifier for which PG is significantly lower than the random guess baseline; i.e., the synthetic data will still expose membership information about the respective targets.

On the 1000 Genomes, PG values have a higher variation overall when the target is chosen randomly from the dataset than for the two smaller HapMap datasets. The results for RBM data confirm our hypothesis that the target’s influence is diluted within larger datasets. However, once again, this does not mean that membership inference is not possible for both Rec-RBM and WGAN, depending on the combination of target, training set, attack classifier, and feature set.

However, in the case of an “extreme” outlier (i.e., a target which has minor alleles at all positions), the synthetic data generated by RBM does not have a big impact on PG. In this case, across all test runs, the PG is actually close to the random guess baseline.

5.2 Privacy Gain under Membership Inference Attack with Partial Information

Next, we introduce a novel attack, which we denote as MIA with Partial Information (MIA-PI). Basically, we only give the attacker access to a fraction of SNVs from the target sequence, chosen at random. The attacker then uses the Recombination model from [48] as an inference method to predict the rest of the sequence. Compared to the previous attack, here the adversary trains their (attack) classifier using the sequence *inferred* from the partial data. Thus, the privacy gain formula also needs to be adjusted to account for how likely an adversary is to identify a target within a dataset from partial information.

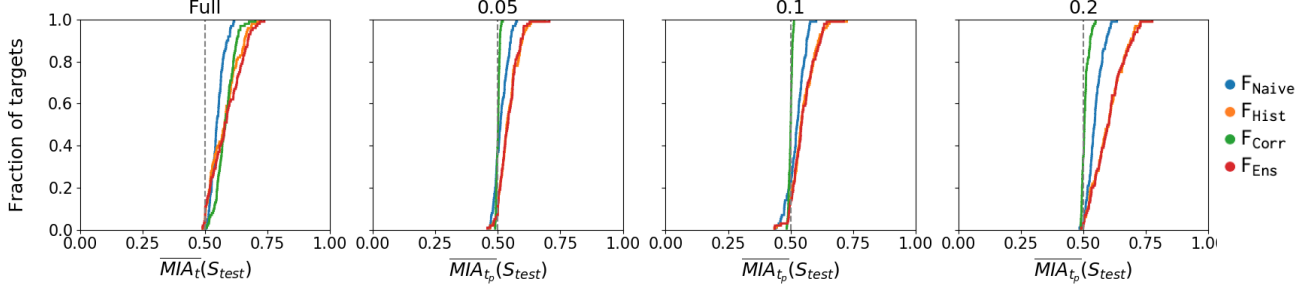


Figure 11: Accuracy of the Membership Inference Attack with access to full sequence and partial information for **Recomb**.

PG for MIA-PI. Assuming the attacker has partial information t' as a fraction of the SNVs from t , they first use the Recomb model, as an inference algorithm, to predict the rest of the SNVs from the target sequence, which we denote by t_p . The privacy gain is computed as $PG_t = \frac{\overline{MIA}_{t_p}(R_t) - \overline{MIA}_{t_p}(S_{test})}{2}$, where $\overline{MIA}_{t_p}(S_{test}) = \sum_{S_i \in S_{test}} \frac{\Pr[MIA_{t_p}(S_i)=1]}{2 \cdot n_s}$ and $\overline{MIA}_{t_p}(R_t) = \sum_{R_i \in R_t} \frac{\Pr[MIA_{t_p}(R_i)=1]}{2 \cdot n_s}$. That is, the privacy gain, in this case, is computed as the difference between the probability that the attacker, who has partial information about the target record, correctly identifies that the target is part of the real dataset versus the target being part of the training set used to generate the synthetic dataset.

As a result, PG now ranges between -0.5 and 0.5, where 0.5 means that having the real dataset R and the partial information t' about the target allows the adversary to infer the membership of t in R , while the synthetic dataset reduces the adversary's chance of success (i.e. $\overline{MIA}_{t_p}(R_t) = 1$ and $\overline{MIA}_{t_p}(S_{test}) = 0$). A negative PG value means that publishing the synthetic data, instead of the real data, improves the adversary's chance to correctly infer membership of the target t (i.e. $\overline{MIA}_{t_p}(R_t) < \overline{MIA}_{t_p}(S_{test})$). If publishing the synthetic data does not increase nor decrease the adversary's inference powers, we should have PG=0 (i.e. $\overline{MIA}_{t_p}(R_t) = \overline{MIA}_{t_p}(S_{test})$).

Experiments. From the experiments above, we find that the attack classifier that yields the lowest PG is Logistic Regression, thus, to ease presentation, we only experiment with that one. In the following, we present the results of the MIA-PI experiments for the CEU population, focusing on the Recomb and RBM models (as mentioned, with a LogReg attack classifier). We do so as these two models yielded the least PG in Section 5.1.

Recomb. In Figure 11, we plot the Cumulative Distribution Function (CDF) of the accuracy of the attack for Recomb when the adversary has access to the full sequence vs. partial information, specifically, a ratio of 0.05, 0.1, and 0.2 of the total SNVs from the target sequence. Interestingly, even when only 0.05 of the target SNVs are available to the attacker, for 90% and 91% of the targets from the Histogram and respectively Ensemble feature sets, the accuracy of the attacker is still above the random guess baseline (50% accuracy). Our intuition is that many targets are vulnerable to the attack, even with little partial information, since we use the Recomb model not only for the attack but also as an inference method to predict the rest of the sequence.

To explore how much of the MIA-PI vulnerability is due to the release of synthetic datasets, and not only by how much information the attacker has available, in Figure 12, we plot the CDF of the PG with MIA-PI. In line with the accuracy results, we find that, in the case of the Correlations feature set, the PG is greater than 0 for at least 88% of the targets, for all ratios of partial information tested. However, for the other three feature sets, releasing the synthetic dataset instead of the real data decreases the privacy gain (i.e., PG<0) for the majority of targets. When the adversary has access to just 5% of the SNVs from the target, there is a negative PG for 61% of the targets under the Histogram and 62% of the targets under the Ensemble feature sets. With 10% of the target sequence available, 54% and 60% of the targets under, respectively, the Histogram and the Ensemble feature sets have negative PG, and with 20% these numbers go up to 64% and 67%. For the Naive feature set, there are more targets with negative PG with increasing partial information available to the attacker, i.e., 59%, 70%, and 84% with, respectively, 5%, 10%, and 20% of the target sequence available. Overall, this shows that releasing the synthetic dataset instead of the synthetic data does not mitigate privacy, even when the attacker does not have access to the full sequence.

RBM. In Figure 13, we plot the CDF for the accuracy of the attack for the RBM model for both full and partial information about the target record available to the attacker. Across all feature sets, there is an increase in the accuracy of the attack with more information available to the attacker, as it is expected. We also look at CDF for the PG in the case of partial information available to the attacker in Figure 14. Once again, under the Naive feature set, increasing the partial information available to the attacker has a negative correlation with the percentage of targets that have a negative PG. Under all other feature sets, for the majority of targets, releasing the synthetic dataset instead of the real data yields a positive PG, meaning that releasing the synthetic dataset instead of the real dataset improves the PG.

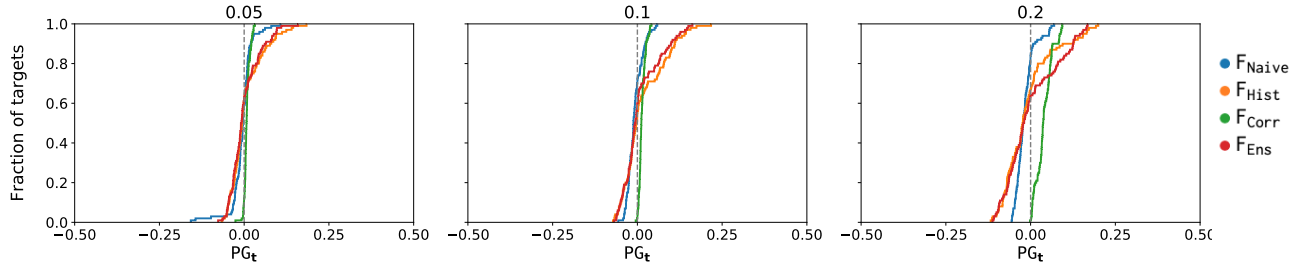


Figure 12: Privacy Gain (PG) for synthetic samples generated by **Recomb**.

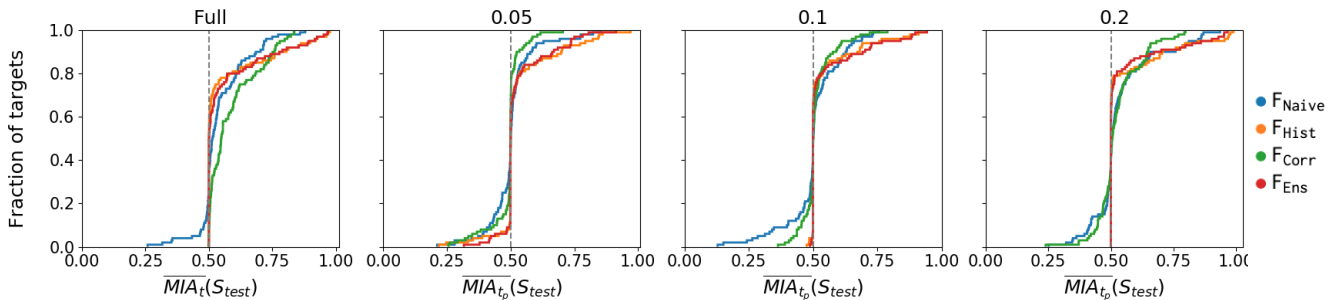


Figure 13: Accuracy of the Membership Inference Attack with access to full sequence and partial information for **RBM**.

Take-Aways. We find that not even decreasing the attacker’s power by only giving him partial information from the target sequence mitigates privacy for the Recomb-generated synthetic data. This is likely due to the fact that, by using the Recomb model as a generative model as well as an inference model, the adversary’s inference power is increased since the feature set extracted from the synthetic data will be closer to the feature set for the predicted target.

However, in this case, for the RBM synthetic data, we see an increase in the privacy gained by releasing synthetic data as opposed to real data. This implies that, even if the RBM is likely to overfit when few samples are available for training, it does so on the predicted sequence of the target rather than on the full sequence, and thus decreases the accuracy of the MIA.

6 Related Work

In this section, we review related work on synthetic data, privacy in genomics, and MIAs against machine learning models.

Synthetic Data Initiatives. In recent years, researchers have focused on the generation of synthetic electronic health records (EHR), aiming to facilitate research in and adoption of machine learning in medicine. Choi et al. [13] use a combination of an autoencoder with GAN model, called medGAN, to generate high-dimensional multi-label discrete data. ADS-GAN [62] uses a quantifiable definition for “identifiability” that is combined with the discriminator’s loss to minimize the probability of patient’s re-identification, while CorGAN [54] combines convolutional GANs and convolutional autoencoders to capture the correlations between adjacent medical features. Biswal et al. [9] use variational autoencoder to synthesize sequences of discrete EHR encounters and encounter features. Other initiatives focus on generating synthetic data modeled on primary care data [3, 41, 56, 60]. Researchers have also explored generating synthetic health patient data to detect cancer and other diseases, e.g., RDP-CGAN [55] combines convolutional GANs and convolutional autoencoders, both trained with Rényi differential privacy [36]. Specific to genomes are the works we have introduced in Section 3 and evaluated, in terms of utility and privacy, throughout the paper [33, 48, 61].

Privacy in Genomics. Researchers have focused on studying and mitigating privacy risks in genomics. One of the first attacks on genomic data is the Membership Inference Attack proposed by Homer et al. [30], showing that an adversary can infer the presence of an individual’s genotype within a complex DNA mixture. This attack has been improved by Wang et al. [58] using correlation statistics of a few hundred SNPs. Then, Im et al. [31] show that the summary information from genome-wide association studies, such as regression coefficients, can also lead to revealing the participation of an individual within the respective study. Membership inference has also been shown possible in the context of the Beacon network [43, 50, 57], a federated service that answers queries of the form “does your data have a specific nucleotide at a specific genomic coordinate?”.

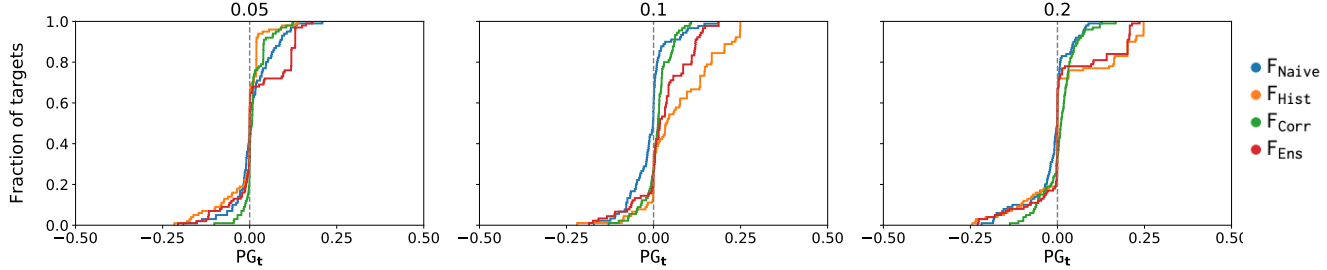


Figure 14: Privacy Gain (PG) for synthetic samples generated by **RBM**.

Close to our work, Chen et al. [12] study the effects of differential privacy protection against membership inference attack on machine learning for genomic data. However, their study is focused on privacy leakage via sharing trained classification models, whereas, we study the privacy leakage from sharing synthetic datasets.

MIAs against Machine Learning Models. Shokri et al. [49] present the first attack against discriminative models, aiming to identify whether a data record was used in training, using an approach based on shadow models. Hayes et al. [24] present the first MIA against generative models like GANs; they use a discriminator to output the data with the highest confidence values as the original training data. Hilprecht et al. [26] study MIAs against both GANs and Variational AutoEncoders (VAEs), while Chen et al. [11] propose a generic MIA model against GANs.

As mentioned, Stadler et al. [53] evaluate MIAs in the context of synthetic data, and show that even access to a single synthetic dataset output by the target model can lead to privacy leakage. We re-use their framework for quantifying the privacy gain when a synthetic dataset is released as opposed to the real dataset. However, not only we do so for a specific context (namely, genomics), but we also measure utility (while they only study privacy) and introduce and measure a novel attack whereby the attacker who only has access to partial genomic information about the target.

Finally, measurement studies have focused on privacy in machine learning. Jayaraman and Evans [32] evaluate differential privacy to understand the impact that different choices for privacy parameters have on both utility and privacy. Long et al. [35] study membership inference attacks on three different discriminative models, in order to understand why and how they succeed.

7 Conclusion

This paper presented an in-depth measurement study of state-of-the-art methods to generate synthetic genomic data. We did so vis-à-vis 1) their utility, with respect to a number of common analytical tasks performed by researchers, as well as 2) the privacy protection they provide compared to releasing real data.

High-quality synthetic data must accurately capture the relations between data points, however, this can enable attackers to infer sensitive information about the training data used to generate the synthetic data. This was illustrated by the performance of the Recomb model on the HapMap datasets: while it achieves the best utility, it does so at the cost of significantly reducing privacy. Overall, there is no single method that outperforms the others for all metrics and all datasets. However, we did find that models based on a simple GAN architecture (i.e., GAN and Rec-GAN) are not a good fit to genomic data, as they provide the lowest utility across the board.

Our analysis revealed that the size of the training dataset matters, especially in the case of generative models. Not only we saw an improvement in utility with the addition of samples in the hybrid Rec-RBM approach for the smaller HapMap datasets, and for RBM and WGAN for the 1000 Genomes dataset, but we also measured a decrease in the number of targets exposed to membership inference.

Our measurement framework can be used by practitioners to assess the risks of deploying synthetic genomic data in the wild, and will serve as a benchmark tool for researchers and practitioners in the future. In future work, we plan to integrate differential privacy mechanisms in our framework, as well as novel metrics and algorithms.

Acknowledgments. This work was partly supported by a Google Faculty Award on “Enabling Progress in Genomic Research via Privacy Preserving Data Sharing” and a grant from the NCSC and the Alan Turing Institute on “Evaluating Privacy-Preserving Generative Models In The Wild.” The authors wish to thank Yang Zhang and Christophe Dessimoz for comments and feedback on the manuscript.

References

- [1] Generating and designing DNA. <https://github.com/co9olguy/Generating-and-designing-DNA>.
- [2] Genetic maps for the 1000 Genomes Project variants. <https://github.com/joepickrell/1000-genomes-genetic-maps>.
- [3] New synthetic datasets to assist COVID-19 and cardiovascular research. <https://www.gov.uk/government/news/new-synthetic-datasets-to-assist-covid-19-and-cardiovascular-research>.
- [4] 1000 Genomes Project Consortium. A global reference for human genetic variation. *Nature*, 526(7571), 2015.
- [5] N. Altman and M. Krzywinski. The curse(s) of dimensionality. *Nature Methods*, 15(6), 2018.
- [6] D. R. Amancio, C. H. Comin, D. Casanova, G. Travieso, O. M. Bruno, F. A. Rodrigues, and L. da Fontoura Costa. A systematic comparison of supervised classifiers. *PloS one*, 9(4):e94137, 2014.
- [7] C. Angermueller, T. Pärnamaa, L. Parts, and O. Stegle. Deep learning for computational biology. *Molecular Systems Biology*, 12(7), 2016.
- [8] E. Ayday, E. De Cristofaro, J.-P. Hubaux, and G. Tsudik. Whole genome sequencing: Revolutionary medicine or privacy nightmare? *Computer*, 48(2), 2015.
- [9] S. Biswal, S. Ghosh, J. Duke, B. Malin, W. Stewart, and J. Sun. EVA: Generating Longitudinal Electronic Health Records Using Conditional Variational Autoencoders. *arXiv:2012.10020*, 2020.
- [10] W. S. Bush and J. H. Moore. Genome-wide association studies. *PLoS Computational Biology*, 8(12), 2012.
- [11] D. Chen, N. Yu, Y. Zhang, and M. Fritz. GAN-Leaks: A taxonomy of membership inference attacks against GANs. In *ACM Conference on Computer and Communications Security*, 2020.
- [12] J. Chen, W. H. Wang, and X. Shi. Differential Privacy Protection Against Membership Inference Attack on Machine Learning for Genomic Data. <https://www.biorxiv.org/content/early/2020/08/04/2020.08.03.235416.full.pdf>, 2020.
- [13] E. Choi, S. Biswal, B. Malin, J. Duke, W. F. Stewart, and J. Sun. Generating multi-label discrete patient records using generative adversarial networks. In *Machine learning for Healthcare Conference*, 2017.
- [14] G. M. Clarke and L. R. Cardon. Disentangling linkage disequilibrium and linkage from dense single-nucleotide polymorphism trio data. *Genetics*, 171(4):2085–2095, 2005.
- [15] E. De Cristofaro. An overview of privacy in machine learning. *arXiv:2005.08679*, 2020.
- [16] H. Elias. Synthetic data - all the perks without the risk? <https://techhq.com/2020/10/synthetic-data-all-the-perks-without-the-risk/>, 2020.
- [17] EMBL-EBI Training. What are genome wide association studies (GWAS)? <https://www.ebi.ac.uk/training-beta/online/courses/gwas-catalogue-exploring-snp-trait-associations/what-is-gwas-catalog/what-are-genome-wide-association-studies-gwas/>, 2021.
- [18] Ensembl Variation. Variant classification. <https://m.ensembl.org/info/genome/variation/prediction/classification.html>, 2020.
- [19] S. N. Evans, Y. Shvets, and M. Slatkin. Non-equilibrium theory of the allele frequency spectrum. *Theoretical Population Biology*, 71(1), 2007.
- [20] R. A. Fisher. The distribution of gene ratios for rare mutations. *Proceedings of the Royal Society of Edinburgh*, 50, 1931.
- [21] Genetics Home Reference. What is Precision Medicine? <https://medlineplus.gov/genetics/understanding/precisionmedicine-definition/>, 2020.
- [22] I. Gulrajani, F. Ahmed, M. Arjovsky, V. Dumoulin, and A. Courville. Improved Training of Wasserstein GANs. In *Advances in Neural Information Processing Systems*, 2017.
- [23] M. Gymrek, A. L. McGuire, D. Golan, E. Halperin, and Y. Erlich. Identifying personal genomes by surname inference. *Science*, 339(6117), 2013.
- [24] J. Hayes, L. Melis, G. Danezis, and E. De Cristofaro. LOGAN: Membership inference attacks against generative models. *Proceedings on Privacy Enhancing Technologies*, 2019.
- [25] K. He, X. Zhang, S. Ren, and J. Sun. Deep Residual Learning for Image Recognition. In *IEEE Conference on Computer Vision and Pattern Recognition*, 2016.
- [26] B. Hilprecht, M. Härterich, and D. Bernau. Monte Carlo and Reconstruction Membership Inference Attacks against Generative Models. *Proceedings on Privacy Enhancing Technologies*, 2019.
- [27] J. L. Hodges. The significance probability of the Smirnov two-sample test. *Arkiv för Matematik*, 3(5), 1958.
- [28] K. E. Holsinger and B. S. Weir. Genetics in geographically structured populations: defining, estimating and interpreting FST. *Nature Reviews Genetics*, 10(9), 2009.
- [29] N. Homer, S. Szelinger, M. Redman, D. Duggan, W. Tembe, J. Muehling, J. V. Pearson, D. A. Stephan, S. F. Nelson, and D. W. Craig. Resolving individuals contributing trace amounts of DNA to highly complex mixtures using high-density SNP genotyping microarrays. *PLoS Genetics*, 4(8), 2008.
- [30] N. Homer, S. Szelinger, M. Redman, D. Duggan, W. Tembe, J. Muehling, J. V. Pearson, D. A. Stephan, S. F. Nelson, and D. W. Craig. Resolving individuals contributing trace amounts of DNA to highly complex mixtures using high-density SNP genotyping microarrays. *PLoS Genetics*, 2008.
- [31] H. K. Im, E. R. Gamazon, D. L. Nicolae, and N. J. Cox. On sharing quantitative trait GWAS results in an era of multiple-omics data and the limits of genomic privacy. *The American Journal of Human Genetics*, 90(4), 2012.
- [32] B. Jayaraman and D. Evans. Evaluating differentially private machine learning in practice. In *USENIX Security*, 2019.

[33] N. Killoran, L. Lee, A. Delong, D. Duvenaud, and B. Frey. Generating and designing DNA with deep generative models. *arXiv:1712.06148*, 2017.

[34] Y. LeCun, B. Boser, J. S. Denker, D. Henderson, R. E. Howard, W. Hubbard, and L. D. Jackel. Backpropagation applied to handwritten zip code recognition. *Neural computation*, 1(4), 1989.

[35] Y. Long, V. Bindschaedler, and C. A. Gunter. Towards measuring membership privacy. *arXiv:1712.09136*, 2017.

[36] I. Mironov. Rényi differential privacy. In *2017 IEEE 30th Computer Security Foundations Symposium (CSF)*, pages 263–275. IEEE, 2017.

[37] A. Mordvintsev, C. Olah, and M. Tyka. Inceptionism: Going Deeper into Neural Networks. <https://ai.googleblog.com/2015/06/inceptionism-going-deeper-into-neural.html>, 2015.

[38] National Human Genome Research Institute. International HapMap Project. <https://www.genome.gov/10001688/international-hapmap-project>, 2012.

[39] National Human Genome Research Institute. Genome-Wide Association Studies Fact Sheet. <https://www.genome.gov/about-genomics/fact-sheets/Genome-Wide-Association-Studies-Fact-Sheet>, 2021.

[40] M. Naveed, E. Ayday, E. W. Clayton, J. Fellay, C. A. Gunter, J.-P. Hubaux, B. A. Malin, and X. Wang. Privacy In The Genomic Era. *ACM Computing Surveys*, 48(1), 2015.

[41] NHS England. A&E Synthetic Data. <https://data.england.nhs.uk/dataset/a-e-synthetic-data>, 2021.

[42] NIH. Genomic Data Sharing. <https://osp.od.nih.gov/scientific-sharing/genomic-data-sharing-faqs/>, 2021.

[43] J. L. Raisaro, F. Tramer, Z. Ji, D. Bu, Y. Zhao, K. Carey, D. Lloyd, H. Sofia, D. Baker, P. Flicek, et al. Addressing beacon re-identification attacks: quantification and mitigation of privacy risks. *Journal of the American Medical Informatics Association*, 24(4):799–805, 2017.

[44] A. R. Rogers and C. Huff. Linkage disequilibrium between loci with unknown phase. *Genetics*, 182, 2009.

[45] A. Sablayrolles, M. Douze, C. Schmid, Y. Ollivier, and H. Jégou. White-box vs Black-box: Bayes Optimal Strategies for Membership Inference. In *International Conference on Machine Learning*, 2019.

[46] P. Sadrach. How Artificial Intelligence Can Revolutionize Healthcare. <https://builtin.com/healthcare-technology/how-ai-revolutionize-healthcare>, 2020.

[47] A. Salem, Y. Zhang, M. Humbert, P. Berrang, M. Fritz, and M. Backes. ML-Leaks: Model and Data Independent Membership Inference Attacks and Defenses on Machine Learning Models. In *Network and Distributed System Security Symposium*, 2019.

[48] S. S. Samani, Z. Huang, E. Ayday, M. Elliot, J. Fellay, J.-P. Hubaux, and Z. Katalik. Quantifying genomic privacy via inference attack with high-order SNV correlations. In *IEEE Security and Privacy Workshops*, 2015.

[49] R. Shokri, M. Stronati, C. Song, and V. Shmatikov. Membership inference attacks against machine learning models. In *IEEE Symposium on Security and Privacy*, 2017.

[50] S. S. Shringarpure and C. D. Bustamante. Privacy risks from genomic data-sharing beacons. *The American Journal of Human Genetics*, 97(5):631–646, 2015.

[51] K. Simonyan, A. Vedaldi, and A. Zisserman. Deep Inside Convolutional Networks: Visualising Image Classification Models and Saliency Maps. *arXiv:1312.6034*, 2013.

[52] P. Smolensky. Information processing in dynamical systems: Foundations of harmony theory. Technical report, Colorado Univ at Boulder Dept of Computer Science, 1986.

[53] T. Stadler, B. Oprisanu, and C. Troncoso. Synthetic Data – A Privacy Mirage. *arXiv:2011.07018*, 2020.

[54] A. Torfi and E. A. Fox. CorGAN: Correlation-capturing convolutional generative adversarial networks for generating synthetic health-care records. *arXiv:2001.09346*, 2020.

[55] A. Torfi, E. A. Fox, and C. K. Reddy. Differentially Private Synthetic Medical Data Generation using Convolutional GANs. *arXiv:2012.11774*, 2020.

[56] A. Tucker, Z. Wang, Y. Rotalinti, and P. Myles. Generating high-fidelity synthetic patient data for assessing machine learning health-care software. *NPJ Digital Medicine*, 3(1), 2020.

[57] N. Von Thenen, E. Ayday, and A. E. Cicek. Re-identification of individuals in genomic data-sharing beacons via allele inference. *Bioinformatics*, 35(3):365–371, 2019.

[58] R. Wang, Y. F. Li, X. Wang, H. Tang, and X. Zhou. Learning your identity and disease from research papers: information leaks in genome wide association study. In *ACM Conference on Computer and Communications Security*, 2009.

[59] S. Wang, X. Jiang, S. Singh, R. Marmor, L. Bonomi, D. Fox, M. Dow, and L. Ohno-Machado. Genome Privacy: Challenges, Technical Approaches to Mitigate Risk, and Ethical Considerations in the United States. *Annals of the New York Academy of Sciences*, 1387(1), 2017.

[60] Z. Wang, P. Myles, and A. Tucker. Generating and Evaluating Synthetic UK Primary Care Data: Preserving Data Utility & Patient Privacy. In *IEEE International Symposium on Computer-Based Medical Systems*, 2019.

[61] B. Yelmen, A. Decelle, L. Ongaro, D. Marnetto, F. Montinaro, C. Furtlechner, L. Pagani, and F. Jay. Creating Artificial Human Genomes Using Generative Models. <https://www.biorxiv.org/content/10.1101/769091v2>, 2019.

[62] J. Yoon, L. Drumright, and M. Schaar. Anonymization Through Data Synthesis Using Generative Adversarial Networks (ADS-GAN). *IEEE Journal of Biomedical and Health Informatics*, PP, 2020.

[63] J. Yosinski, J. Clune, A. Nguyen, T. Fuchs, and H. Lipson. Understanding Neural Networks Through Deep Visualization. *arXiv:1506.06579*, 2015.

[64] X. Zhou, B. Peng, Y. F. Li, Y. Chen, H. Tang, and X. Wang. To release or not to release: evaluating information leaks in aggregate human-genome data. In *European Symposium on Research in Computer Security*, pages 607–627. Springer, 2011.